JACS
JOURNAL OF THE AMERICAN CHEMICAL SOCIETY
pubs.acs.org/JACS
Article

Dinitrogen Cleavage by a Heterometallic Cluster Featuring Multiple Uranium–Rhodium Bonds

Xiaoqing Xin, Iskander Douair, Yue Zhao, Shuao Wang, Laurent Maron,* and Congqing Zhu*

Cite This: J. Am. Chem. Soc. 2020, 142, 15004–15011
Read Online

ABSTRACT: Reduction of dinitrogen (N_2) is a major challenge for chemists. Cooperation of multiple metal centers to break the strong N_2 triple bond has been identified as a crucial step in both the industrial and the natural ammonia syntheses. However, reports of the cleavage of N_2 by a multimetallic uranium complex remain extremely rare, although uranium species were used as catalyst in the early Harber–Bosch process. Here we report the cleavage of N_2 to two nitrides by a multimetallic uranium–rhodium cluster at ambient temperature and pressure. The nitride product further reacts with acid to give substantial yields of ammonium. The presence of uranium–rhodium bond in this multimetallic cluster was revealed by X-ray crystallographic and computational studies. This study demonstrates that the multimetallic clusters containing uranium and transition metals are promising materials for N_2 fixation and reduction.

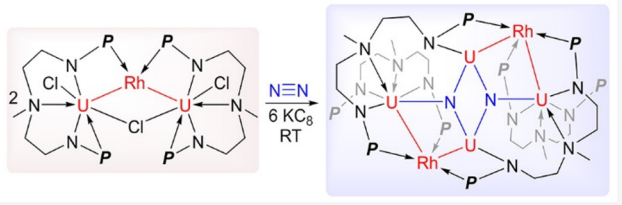

INTRODUCTION

The cleavage and conversion of the strong N≡N triple bond in dinitrogen (N_2) have attracted considerable attention from both academia and industry.[1−12] The current industrial ammonia synthesis from N_2, the Haber–Bosch process, uses an iron-based catalyst and requires high temperatures and pressures. Biologically, however, N_2 can be converted to ammonia by nitrogenases at ambient temperature and pressure. The most important active site in nitrogenases is a multimetallic iron–molybdenum cluster.[13−16] This has inspired chemists to explore the fixation and reduction of N_2 by Fe- and Mo-based molecular catalysts, which have been investigated extensively in recent decades.[17−28]

Before an Fe-based catalyst was used for the industrial synthesis of ammonia, the early Haber–Bosch process utilized a uranium-based catalyst.[29] Since the first uranium N_2 complex was reported in 1998,[30] some examples of molecular uranium complexes capable of fixing or reducing N_2 have appeared.[31−40] However, only one example of N_2 cleavage achieved by a uranium species with [K(naphthalenide)] has been reported.[33] Consequently, understanding the six-electron N_2 reduction by molecular uranium complexes remains a substantial challenge.[41] Previous investigations show that the multimetallic uranium complexes have great potential in N_2 reduction due to the synergistic effects from the different metals.[31,36−38] For instance, Cummins and co-workers showed that a trivalent uranium precursor can facilitate N_2 reduction on a Mo center.[31] Mazzanti and co-workers reported a four-electron reduction of N_2 by the multimetallic uranium–potassium complexes.[36,37] Very recently, Arnold and co-workers reported that thorium or uranium dinuclear metallacycles can mediate the four-electron reduction and conversion of N_2 in the presence of KC_8.[40] These studies suggest that dinitrogen fixation or activation may be expected for highly active low-valent uranium compounds with N/O-donor-based ligand. However, the complete cleavage of N_2, a six-electron reduction, by multimetallic complexes containing uranium and transition metals has not been reported to date.

Here we describe the first example of a multimetallic uranium–rhodium cluster that reacts with N_2 and a potassium-based reducing agent to give a species with two nitrides through N≡N bond cleavage. Protonation of this product with an excess of acid leads to the formation of ammonium.

RESULTS AND DISCUSSION

Synthesis, Characterization, and Reactivity. Complex {U[N(CH_3)($CH_2CH_2NP^iPr_2$)$_2$](Cl)$_2$(THF)} (**2**) was synthesized by the reaction of uranium tetrachloride (UCl_4) with [$CH_3N(CH_2CH_2NHP^iPr_2)_2$] (**1**) in the presence of ^{n}BuLi in tetrahydrofuran (THF). It can be isolated as a brown solid in 82% yield (Scheme 1). The structure of **2** was characterized by nuclear magnetic resonance (NMR) spectroscopy, elemental analysis, and single-crystal X-ray diffraction. The ^{1}H NMR spectrum of **2** shows a broad range of peaks from +88.49 to −81.53 ppm, which is consistent with the presence of paramagnetic tetravalent uranium complexes. Our previous

Received: May 28, 2020
Published: August 7, 2020

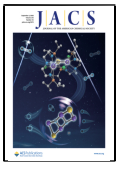

https://dx.doi.org/10.1021/jacs.0c05788
J. Am. Chem. Soc. 2020, 142, 15004−15011

Scheme 1. Cleavage of N_2 by a Multimetallic Uranium−Rhodium Cluster

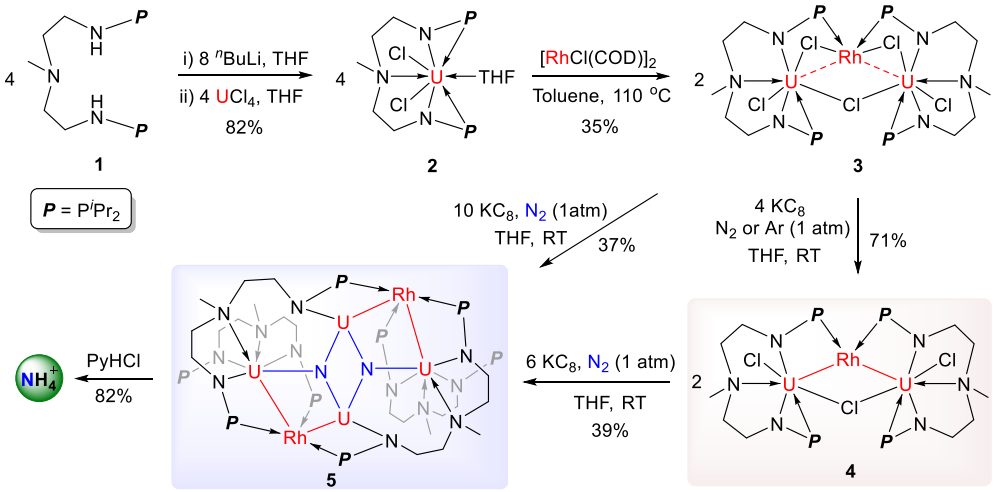

studies implied that complexes with the N−P ligand are useful precursors for the construction of multimetallic clusters with *f*-block elements.[42−45] Therefore, we examined the reaction of **2** with monovalent transition metal species. Treatment of 4 equiv of monomeric uranium complex **2** with 1 equiv of $[RhCl(COD)]_2$ (COD = cyclooctadiene) at 110 °C in toluene results in the formation of a complex $[\{U[N(CH_3)(CH_2CH_2NP^iPr_2)_2](Cl_2)\}_2(\mu\text{-Cl})(\mu\text{-Rh})]$ (**3**) as brown crystals in 35% yield after recrystallization from toluene at −30 °C (Scheme 1).

The reduction of 2 equiv of complex **3** with 4 equiv of potassium graphite (KC_8) in THF under 1 atm of N_2 or argon leads to the formation of a multimetallic cluster $[\{U[N(CH_3)(CH_2CH_2NP^iPr_2)_2](Cl)\}_2(\mu\text{-Cl})(\mu\text{-Rh})]$ (**4**), which can be isolated as red-brown crystals in 71% yield after a simple workup (Scheme 1). Further reduction of 2 equiv of complex **4** with 6 equiv of KC_8 under a N_2 atmosphere (1 atm) for 2 h followed by filtration and recrystallization furnished the N_2 cleavage complex $[\{U_2[N(CH_3)(CH_2CH_2NP^iPr_2)_2]_2(Rh)(\mu\text{-N})\}_2]$ (**5**) in 39% yield as dark brown crystals (Scheme 1). The deep colors of these multimetallic uranium clusters (**3**, **4**, and **5**) are consistent with the strong absorption of their THF solution in the ultraviolet−visible region (Figures S12−S14).

Complex **5** can be prepared directly by the reduction of 2 equiv of complex **3** with an excess (typically 10 equiv) of KC_8 under 1 atm of N_2 at RT for 6 h. From *in situ* NMR experiments, we found that only complex **4** was generated in the first 2 h and could further react with the residual KC_8 to form the final N_2 cleavage product **5** (Figure S8). In addition, the reaction of complex **2** with excess KC_8 in THF under 1 atm of N_2 at RT for 2 days was performed, and no reaction occurred, which suggests that this tetravalent uranium complex **2** was not liable to be reduced by KC_8, affording low-valent uranium species and then to reduce the N_2. Therefore, the cluster **4** with U−Rh bonds is the species which undergoes the N_2 cleavage in the presence of KC_8. Only a mixture of unidentified products was observed with reduction of 2 equiv of complexes **3** or **4** with 10 or 6 equiv of KC_8 under an atmosphere of argon rather than N_2. These results demonstrate that the two nitride ligands in **5** originate from N_2.

To further verify the source of the nitride in complex **5**, the ^{15}N-labeled product, **5**-^{15}**N**, was synthesized by the reduction of **3** with KC_8 under 1 atm of $^{15}N_2$. The production of the ammonium ion, NH_4^+, was observed by the acidification of these N_2 cleavage products, **5** and **5**-^{15}**N** (Figures S9−S11). For instance, treatment of a THF solution of **5** with 50 equiv of pyridine hydrochloride (PyHCl) gives NH_4Cl in 82% yield, which shows a triplet resonance (δ = 7.32 ppm, J_{NH} = 52 Hz) in its ^1H NMR spectrum in deuterated dimethyl sulfoxide. Under the same procedure, a doublet resonance (δ = 7.32 ppm, J_{NH} = 72 Hz) was observed in the ^1H NMR spectrum for the acidified product, $^{15}NH_4Cl$, formed from **5**-^{15}**N**. These results are consistent with previous studies for N_2 reduction and hydrogenation to ammonia.[22,36] These ^{15}N-labeled studies demonstrate that the two nitride ligands in **5** originate from N_2 and that both the nitrides are nucleophilic and react with acid to form ammonium salts. Therefore, the formation of **5** from **3** or **4** involves the binding, activation, and complete six-electron reductive cleavage of N_2 by a multimetallic uranium−rhodium cluster and KC_8 under conditions of ambient temperature and pressure. Encouraged by the achievements of uranium nitride functionalization,[36,41,46−50] the attempt to synthesize N-containing organic compounds from complex **5** was unsuccessful thus far.

The variable-temperature magnetic data of complexes **2**, **3**, **4**, and **5** were measured in the solid state with a superconducting quantum interference device (SQUID). The magnetic moments for these complexes exhibit a strong temperature dependency and approach to zero at low temperatures (Figures S16−S19). These results show that the formal oxidation state of U ions in these clusters is +IV. Due to the unique electronic structure in our system, the NIR data for complexes **3**, **4**, and **5** (Figure S15) do not resemble typical U(IV) complexes[51−53] but are more similar to electronically noninnocent systems.[54,55] Therefore, the reduction of 2 equiv of complex **3** with 4 equiv of KC_8 has the effect of reducing Rh(I) to Rh(−I), whereas the six reducing electrons were used to cleavage the N≡N triple bond in the formation of **5** from the reaction of 2 equiv of complex **4** with 6 equiv of KC_8. Thus, the formal oxidation states of U and Rh (+IV for U and −I for Rh) in both clusters **4** and **5** are identical. To the best of our knowledge, this is the first example of six-electron reduction of N_2 by a multimetallic cluster with a uranium−metal bond and a reducing agent (KC_8).

Solid-State Structures. The solid-state structures of complexes **2**, **3**, **4**, and **5** were determined by X-ray

https://dx.doi.org/10.1021/jacs.0c05788
J. Am. Chem. Soc. 2020, 142, 15004−15011

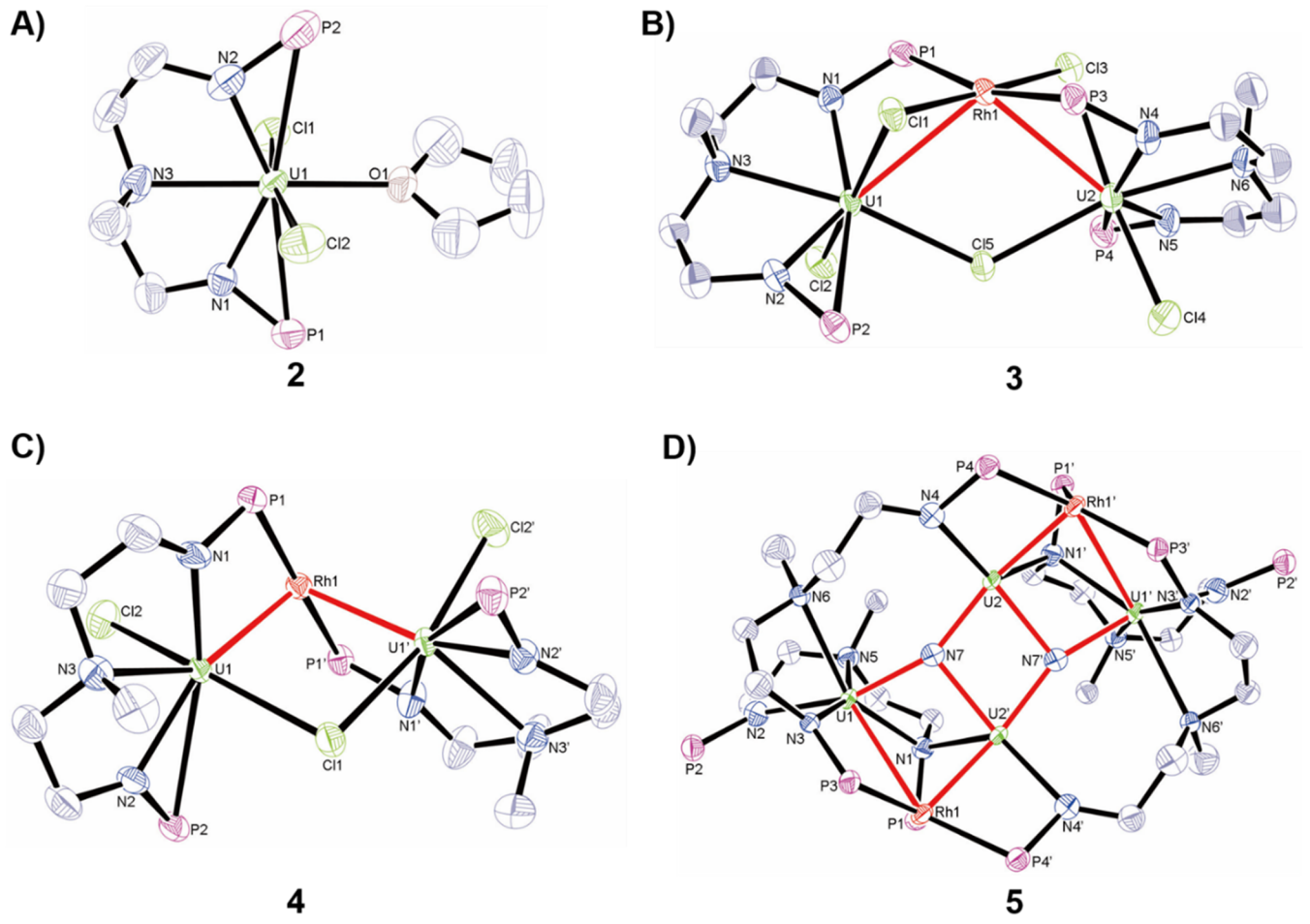

Figure 1. Solid-state structures of **2** (**A**), **3** (**B**), **4** (**C**), and **5** (**D**) by X-ray crystallography with 50% probability ellipsoids. Solvent molecules, hydrogen atoms, and isopropyl moieties in P^iPr_2 are omitted for clarity. The U−Rh bonds in **3** and **4** and the core of **5** ($U_4Rh_2N_2$) are red. Uranium, green; rhodium, red; phosphorus, violet red; nitrogen, blue; chlorine, yellow green; oxygen, pink; and carbon, gray.

crystallography (Figure 1). The structural features of complex **2** were very similar to the uranium species employing a dianionic N−P ligand, $\{O[(CH_2)_2NP(^iPr)_2]_2UCl_2(THF)\}$.[45] The U−Rh distances of 3.3177(5) Å and 3.2609(5) Å in complex **3** are larger than the sum of the covalent single bond radii for uranium and rhodium (2.95 Å),[56] which suggests that weak bonding interactions between Rh and U exist in complex **3** (Figure 1B).

However, the U−Rh distances in complex **4** (2.6555(6) Å) are significantly shorter than those found in complex **3** (Figure 1C). This U−Rh bond length is also shorter than the previously reported U−Rh dative bonds (2.7601(5) and 2.7630(5) Å) but slightly longer than the U−Rh double dative bond (2.5835(3) Å).[57,58] The U1···U1′ separation of 4.0397(6) Å suggests that there is no significant U−U bonding interaction—the sum of the covalent single bond radii for U is 3.40 Å. With the formal oxidation states of U(IV) and Rh(−I) in complex **4**, the bonding of the U−Rh−U unit probably has two resonance structures, U1−Rh1 → U1′ and U1 ← Rh1−U1′, both of which contain a U−Rh σ bond and a Rh-to-U dative bond (Figure S20).

The centrosymmetric structure of **5** reveals the presence of two bridged nitride groups (N^{3-}) in a $U_4Rh_2N_2$ core (Figure 1D). Each of the nitride atoms is bonded to three U atoms, with one U−N bond (U2′−N7: 2.302(6) Å) being significantly longer than the other two almost equivalent U−N bonds (U1−N7: 2.158(7) and U2−N7: 2.154(7) Å). These three U−N bond distances in complex **5** are comparable to those found in a hydrazido-bridged uranium complex (2.163(13)−2.311(13) Å)[36] and are consistent with the presence of U−N single bonds. The N7···N7′ distance of 2.780 Å in complex **5** suggests that there is no N−N bond. Thus, the N≡N triple bond in N_2 has been broken via a six-electron reduction to form two nitrides. Previous studies show that the four-electron reductive cleavage of the N=N double bond in azobenzene to form bisphenylimido derivatives has been established by electron-rich uranium species with redox-active ligands.[59,60]

The U2′−Rh1 bond length of 2.5139(7) Å in complex **5** is slightly shorter than that found in complex **4**, which is consistent with a direct U−Rh σ bond. However, the bond length of U1−Rh1 (3.2160(7) Å) is much longer than the sum of the covalent single bond radii for U and Rh (2.95 Å),[56] suggesting a weak dative bond interaction between Rh1 and U1. In addition, the distances of U1···U2′ (3.4677(4) Å) and U2···U2′ (3.4730(6) Å) are shorter than that in **4**, indicating a weak interaction between these U atoms. Despite a series of species with U−M bonds reported previously,[61−68] the formation of complex **5** is the first example of N_2 fixation, reduction, and cleavage by a complex containing U−M bonds.

Computational Analysis. To gain further insight into the nature of this unprecedented full reduction of N_2, DFT

https://dx.doi.org/10.1021/jacs.0c05788
J. Am. Chem. Soc. 2020, 142, 15004−15011

(B3PW91 with and without inclusion of the dispersion corrections) calculations were carried out to describe the bonding in complexes **3**, **4**, and **5** as this computational approach has proven its accuracy to describe U−M systems.[42,43] The optimized geometry of complex **3** with dispersion correction included is in excellent agreement with the experimental one (see Supporting Information). Among other things, the U−Rh bond distances are reproduced with an accuracy of 0.01 Å (3.28 and 3.31 Å) as well as the U−Cl and Rh−Cl bond lengths, illustrating the correctness of this method. The square planar geometry around the rhodium center is consistent with a Rh(I) d^8 center, implying the presence of two U(IV) moieties. The latter is ensured by the unpaired density plot (see Supporting Information). Even though the U−Rh distance is long, a bonding interaction is observed in the molecular orbital spectrum. Indeed, the HOMO−6 (Figure 2) shows a bonding interaction between the two uranium centers and the rhodium. This orbital is strongly polarized toward Rh (95%) and can be viewed as a donation from a filled d orbital of Rh to the empty df hybrid orbitals on U (5%). On the other hand, no U−U interaction could be found.

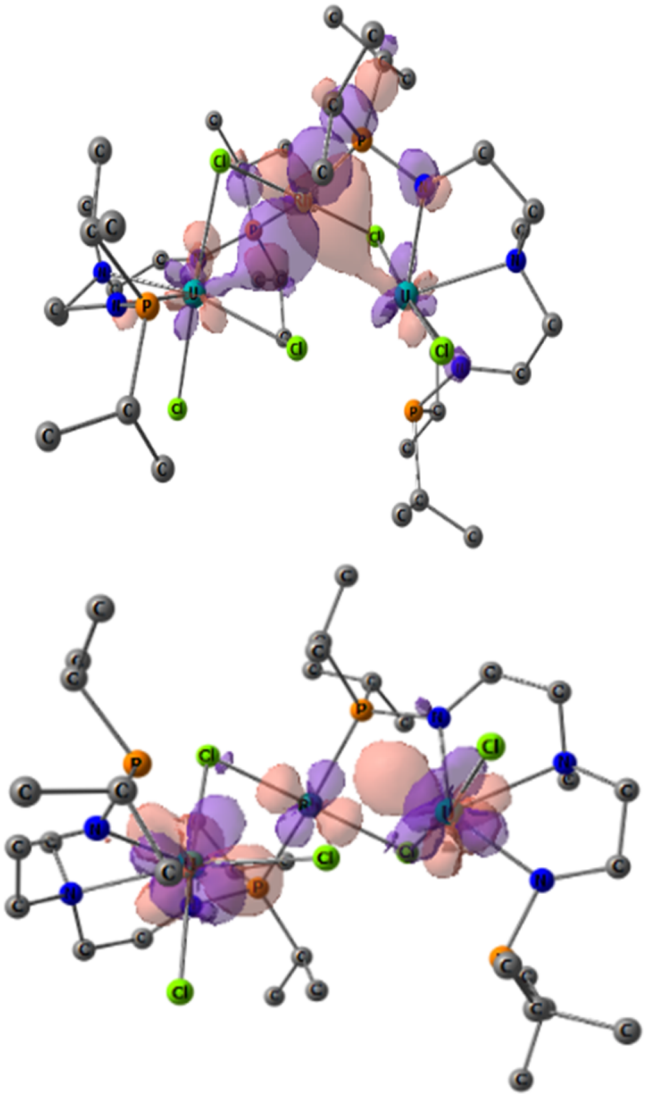

Figure 2. Selected molecular orbitals of complex **3**. The HOMO−6 displaying the U−Rh bonding interaction is on the top and the LUMO on the bottom.

This description is corroborated by the natural bonding orbital (NBO) analysis in which donations from Rh to U are found at the second-order donor−acceptor level (donation around 40 kcal mol^{-1}). Interestingly, some back-donation U−Rh was also found (20 kcal mol^{-1} in average), enhancing the presence of a Rh(I) d^8. The LUMO of the system (Figure 2) involves the empty d orbital on Rh as well as f orbitals on the two uranium centers. Consequently, the reduction of complex **3** can involve both the uranium and rhodium centers. To investigate this, calculations were carried out on complex **4**, which was obtained by reacting **3** with 2 equiv of KC_8. Similar to complex **3**, the optimized geometry of **4** with dispersion correction included is in agreement with the experimental geometry. The shortening of the U−Rh distance is observed, and the distance is reproduced with a precision of 0.05 Å. The short distance is in line with a more covalent interaction as found both in the molecular orbital diagram and at the NBO level.

Two σ U−Rh interactions strongly polarized toward Rh (91%) are found and involve a pure d orbital on Rh (97%) and a pdf hybrid orbital on U (12% p, 35% d, and 49% f). The associated WBIs are 0.85, in line with mainly covalent interactions (donor−acceptor interaction with overlap). On the other hand, some U−U interaction is observed as indicated by a WBI of 0.17 (equivalent to hydrogen bonding). The geometry around Rh is no longer square-planar but rather a distorted tetrahedron that may indicate that the reduction mainly occurred at the rhodium center having a d^{10} configuration. This is confirmed by analysis of the unpaired spin density (Figure 3). Indeed, the unpaired spin density is only located on the two uranium centers, consistent with a closed-shell configuration at the Rh center, and the values that were found are similar to that of complex **3**, in line with two U(IV). Thus, the reduction occurred at the Rh center. This is further highlighted by a large core calculation where the oxidation state of uranium was fixed to +IV (the optimized geometry in this case compares well with the small core one;

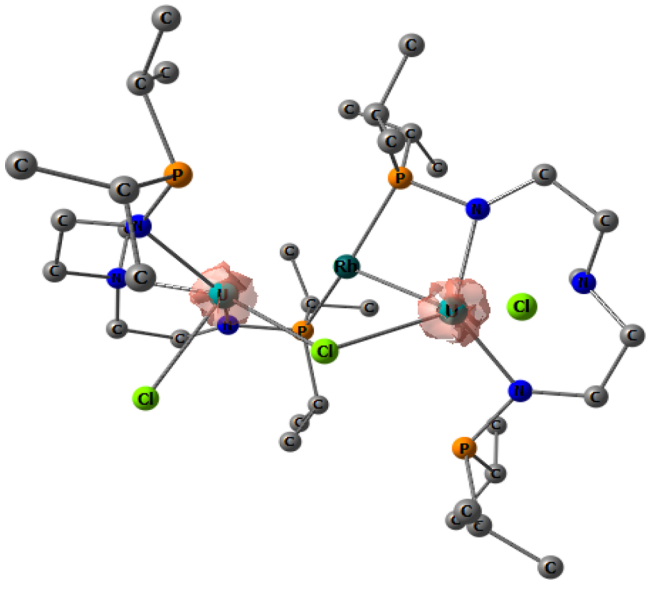

Figure 3. Unpaired spin density plot of complex **4**.

https://dx.doi.org/10.1021/jacs.0c05788
J. Am. Chem. Soc. 2020, 142, 15004−15011

see table in the theoretical calculations section in the SI). Interestingly, although the U−Rh distances are far less precise without dispersion corrections, the bonding analysis is quite similar in terms of interactions but not in strength.

Finally, the unprecedented reduction of N_2 by complex **4** was investigated computationally, even though locating transition states for a heterometallic cluster electron transfer reaction is not possible as it occurs through tunneling effects. It should be noticed that experimentally in the absence of Rh the reduction of N_2 does not occur, and this is consistent with a cooperative effect between the two metals. As the Rh centers in complex **4** are already fully reduced, the subsequent reduction of N_2 should involve the uranium center. This is highlighted by the nature of the LUMO of complex **4** (Figure 4), that is,

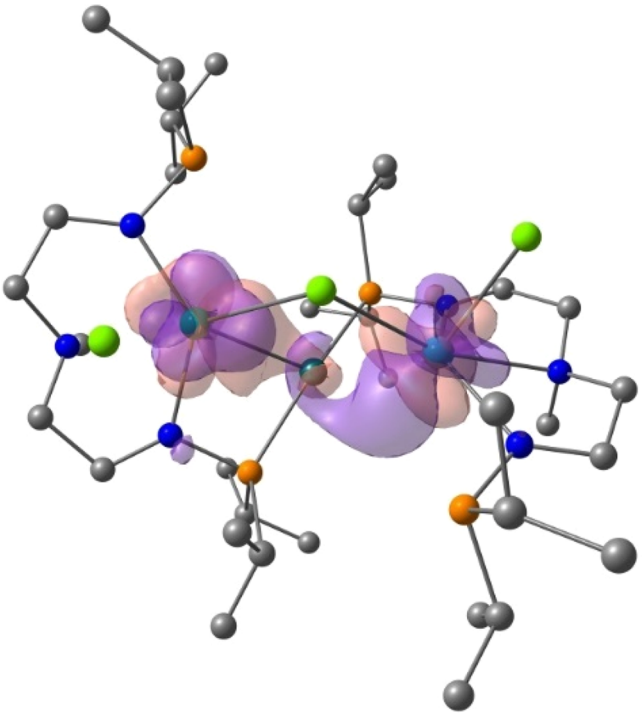

Figure 4. LUMO of complex **4**.

involving the two uranium centers but also the rhodium. Therefore, the coordination of an incoming molecule such as N_2 has to occur at the uranium center, and the electron-rich rhodium ensures electronic stabilization through electronic communication with the uranium centers.

Accordingly, a possible reaction sequence is proposed in which N_2 is sequentially reduced with 6 equiv of KC_8 to abstract the chlorine ions (Figure 5). The overall reduction of N_2 from **4** to **5** is exothermic by 40.0 kcal mol^{-1}, and each step of this reduction is computed to be favored (23.4 kcal mol^{-1} for the formation of **A** from **4** and 6.3 kcal mol^{-1} for the formation of **B** from **A** and finally 10.3 kcal mol^{-1} for the formation of **5** from **B**). This process is similar to that observed in the formation of **4** from **3** which is exothermic by 17.6 kcal mol^{-1}. The reduction of N_2 is effective through the coordination to the uranium centers in the proposed intermediates as highlighted by the increase of the N−N bond distance (1.23 Å in **A** in line with a double bond character and 1.43 Å in **B** in line with a single bond). Moreover, the disruption of the N−N bond is evidenced by the nature of the HOMO of intermediates **A** and **B** (see Supporting Information). For intermediate **A**, the HOMO is clearly the N−N π^* in line with the disruption of one N−N π bond. The LUMO is the second π^* that overlaps with f orbitals on uranium and involves a d from Rh. Thus, this indicates that a second reduction of the N−N bond would be possible by populating this LUMO, and this reduction will involve both uranium and rhodium centers. This second reduction is therefore found in the molecular orbital diagram of intermediate **B**, as the HOMO is the second N−N π^* in line with a sequential disruption of the N−N bond. The HOMO is clearly involving both a uranium and rhodium center in line with a cooperative effect of the two metals for this reduction. The LUMO of intermediate **B** involves the σ^* of N_2 but also the rhodium and uranium centers so that a further reduction of N_2 is possible and implies U and Rh. This is achieved in complex **5** for which the HOMO in this time only involves the rhodium center that further highlights the importance of the rhodium center in this reduction process.

Due to the number of metal centers, calculations of complex **5** were conducted using f-in-core RECPs to describe the uranium centers adapted to the +IV oxidation state. The optimized geometry using this methodology is in agreement with the experimental geometry (see Supporting Information). The U−U distance is well reproduced within 2.0%, and the U−Rh bond length is reproduced with a maximum deviation of 9.0%. The latter is well-known when large RECPs are used as it corresponds to the lack of correlation of the core−valences. Thus, these results are in line with an oxidation state +IV of the uranium centers and −I of the rhodium in complex **5**. This is further corroborated by small core calculations of unpaired spin densities (2.0 on each U, see Supporting Information). The bonding analysis in complex **5** indicates that the U−Rh bonds are mainly described as dative bonds from filled d orbitals on Rh into an empty df hybrid orbital on the U. This is further highlighted by the WBIs which are 0.52 and

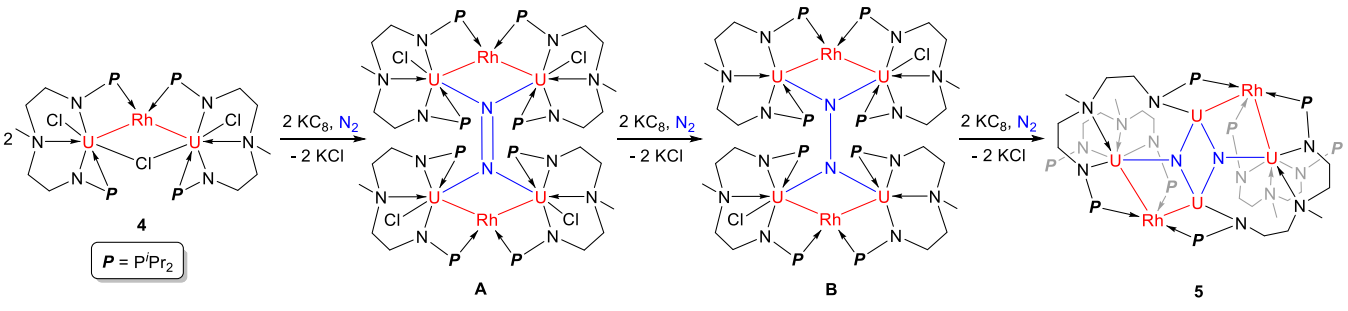

Figure 5. Proposed reaction sequence for the N_2 reduction.

https://dx.doi.org/10.1021/jacs.0c05788
J. Am. Chem. Soc. 2020, 142, 15004−15011

0.35 in line with a less covalent interaction than in complex **4** (for comparison the U−Rh WBI is 0.83 in complex **4**). A weak U−U interaction is also found with an associated WBI of 0.25, whereas no N−N interaction is observed and the LUMO of the system is a π-type interaction between the two nitrogen centers, in line with a fully cleaved N−N bond.

CONCLUSION

In summary, we have shown that the multimetallic uranium−rhodium cluster can be used to cause the cleavage of N_2 in the presence of KC_8. Although uranium complexes exhibit great potential in N_2 reduction, the complete cleavage of N_2 by a multimetallic uranium complex remains extremely rare. Therefore, the formation of N_2 cleavage product **5** from **3** or **4** represents the first example of N_2 fixation and six-electron reduction by a multimetallic cluster with uranium and transition metals. The ^{15}N-labeled product (**5**-^{15}**N**) was synthesized from $^{15}N_2$, further confirming the two nitride ligands in complex **5** originated from N_2. The nitride products **5** and **5**-^{15}**N** could be protonated by excess acid, leading to the formation of substantial yields of ammonia. Computational analysis indicates that the cooperation of uranium and rhodium is important in this process of N_2 cleavage, as after the reduction of the rhodium center the N_2 molecule can be reduced by KC_8 with the help of the uranium center. This study demonstrates that a multimetallic uranium cluster can serve as an efficient platform for N_2 fixation and reduction. Further studies on the mechanism of N_2 reduction by **4** and the functionalization of **5** are in progress.

ASSOCIATED CONTENT

Supporting Information

The Supporting Information is available free of charge at https://pubs.acs.org/doi/10.1021/jacs.0c05788.

Complete experimental details, NMR and electronic absorption spectrum, SQUID, and computational details including Cartesian coordinates, and crystallographic data (PDF)

Crystallographic data for **2** (CIF)

Crystallographic data for **3** (CIF)

Crystallographic data for **4** (CIF)

Crystallographic data for **5** (CIF)

AUTHOR INFORMATION

Corresponding Authors

Laurent Maron − *LPCNO, CNRS & INSA, Université Paul Sabatier, 31077 Toulouse, France;* orcid.org/0000-0003-2653-8557; Email: laurent.maron@irsamc.ups-tlse.fr

Congqing Zhu − *State Key Laboratory of Coordination Chemistry, Jiangsu Key Laboratory of Advanced Organic Materials, School of Chemistry and Chemical Engineering, Nanjing University, Nanjing 210023, China;* orcid.org/0000-0003-4722-0484; Email: zcq@nju.edu.cn

Authors

Xiaoqing Xin − *State Key Laboratory of Coordination Chemistry, Jiangsu Key Laboratory of Advanced Organic Materials, School of Chemistry and Chemical Engineering, Nanjing University, Nanjing 210023, China*

Iskander Douair − *LPCNO, CNRS & INSA, Université Paul Sabatier, 31077 Toulouse, France*

Yue Zhao − *State Key Laboratory of Coordination Chemistry, Jiangsu Key Laboratory of Advanced Organic Materials, School of Chemistry and Chemical Engineering, Nanjing University, Nanjing 210023, China;* orcid.org/0000-0001-6094-4087

Shuao Wang − *State Key Laboratory of Radiation Medicine and Protection, School for Radiological and Interdisciplinary Sciences (RAD-X) and Collaborative Innovation Center of Radiation Medicine of Jiangsu Higher Education Institutions, Soochow University, Suzhou, China;* orcid.org/0000-0002-1526-1102

Complete contact information is available at: https://pubs.acs.org/10.1021/jacs.0c05788

Notes

The authors declare no competing financial interest.

ACKNOWLEDGMENTS

This research was supported by the National Natural Science Foundation of China (Grant Nos. 21772088 and 91961116), the Fundamental Research Funds for the Central Universities (14380216), the Young Elite Scientist Sponsorship Program of China Association of Science and Technology, the program of Jiangsu Specially-Appointed Professor, and Shuangchuang Talent Plan of Jiangsu Province. The authors thank Dr. Tianwei Wang at Nanjing University for assistance with SQUID experiments. L.M. is a member of the Institut Universitaire de France. The Humboldt Foundation and Chinese Academy of Science are acknowledged for support. CalMip is also gratefully acknowledged for a generous grant of computing time.

REFERENCES

(1) Schlögl, R. Ammonia Synthesis. In *Handbook of Homogeneous Catalysis*; Ertl, G., Knözinger, H., Schüth, F., Weitkamp, J., Eds.; Wiley, 2008.

(2) MacKay, B. A.; Fryzuk, M. D. Dinitrogen coordination chemistry: on the biomimetic borderlands. *Chem. Rev.* **2004**, *104*, 385−402.

(3) Burford, R. J.; Fryzuk, M. D. Examining the relationship between coordination mode and reactivity of dinitrogen. *Nat. Rev. Chem.* **2017**, *1*, 0026.

(4) Chen, J. G.; Crooks, R. M.; Seefeldt, L. C.; Bren, K. L.; Bullock, R. M.; Darensbourg, M. Y.; Holland, P. L.; Hoffman, B.; Janik, M. J.; Jones, A. K.; Kanatzidis, M. G.; King, P.; Lancaster, K. M.; Lymar, S. V.; Pfromm, P.; Schneider, W. F.; Schrock, R. R. Beyond fossil fuel−driven nitrogen transformations. *Science* **2018**, *360*, eaar6611.

(5) Foster, S. L.; Bakovic, S. I. P.; Duda, R. D.; Maheshwari, S.; Milton, R. D.; Minteer, S. D.; Janik, M. J.; Renner, J. N.; Greenlee, L. F. Catalysts for nitrogen reduction to ammonia. *Nat. Catal.* **2018**, *1*, 490−500.

(6) Pool, J. A.; Lobkovsky, E.; Chirik, P. J. Hydrogenation and cleavage of dinitrogen to ammonia with a zirconium complex. *Nature* **2004**, *427*, 527−530.

(7) Knobloch, D. J.; Lobkovsky, E.; Chirik, P. J. Dinitrogen cleavage and functionalization by carbon monoxide promoted by a hafnium complex. *Nat. Chem.* **2010**, *2*, 30−35.

(8) Shima, T.; Hu, S.; Luo, G.; Kang, X.; Luo, Y.; Hou, Z. Dinitrogen cleavage and hydrogenation by a trinuclear titanium polyhydride complex. *Science* **2013**, *340*, 1549−1552.

(9) Gao, Y.; Li, G.; Deng, L. Bis(dinitrogen)cobalt(−1) complexes with NHC ligation: Synthesis, characterization, and their dinitrogen functionalization reactions affording side-on bound diazene complexes. *J. Am. Chem. Soc.* **2018**, *140*, 2239−2250.

(10) Légaré, M.-A.; Rang, M.; Bélanger-Chabot, G.; Schweizer, J. I.; Krummenacher, I.; Bertermann, R.; Arrowsmith, M.; Holthausen, M.

C.; Braunschweig, H. The reductive coupling of dinitrogen. *Science* **2019**, *363*, 1329−1332.
(11) Lv, Z.-J.; Huang, Z.; Zhang, W.-X.; Xi, Z. Scandium-promoted direct conversion of dinitrogen into hydrazine derivatives via N−C bond formation. *J. Am. Chem. Soc.* **2019**, *141*, 8773−8777.
(12) Yin, J.; Li, J.; Wang, G.-X.; Yin, Z.-B.; Zhang, W.-X.; Xi, Z. Dinitrogen functionalization affording chromium hydrazido complex. *J. Am. Chem. Soc.* **2019**, *141*, 4241−4247.
(13) Einsle, O.; Tezcan, F. A.; Andrade, S. L. A.; Schmid, B.; Yoshida, M.; Howard, J. B.; Rees, D. C. Nitrogenase MoFe-protein at 1.16 Å resolution: a central ligand in the FeMo-cofactor. *Science* **2002**, *297*, 1696−1700.
(14) Spatzal, T.; Aksoyoglu, M.; Zhang, L.; Andrade, S. L. A.; Schleicher, E.; Weber, S.; Rees, D. C.; Einsle, O. Evidence for interstitial carbon in nitrogenase FeMo cofactor. *Science* **2011**, *334*, 940.
(15) Lancaster, K. M.; Roemelt, M.; Ettenhuber, P.; Hu, Y.; Ribbe, M. W.; Neese, F.; Bergmann, U.; DeBeer, S. X-ray emission spectroscopy evidences a central carbon in the nitrogenase iron-molybdenum cofactor. *Science* **2011**, *334*, 974−977.
(16) Hoffman, B. M.; Lukoyanov, D.; Yang, Z. Y.; Dean, D. R.; Seefeldt, L. C. Mechanism of nitrogen fixation by nitrogenase: the next stage. *Chem. Rev.* **2014**, *114*, 4041−4062.
(17) Laplaza, C. E.; Cummins, C. C. Dinitrogen cleavage by a three-coordinate molybdenum(III) complex. *Science* **1995**, *268*, 861−863.
(18) Yandulov, D. V.; Schrock, R. R. Catalytic reduction of dinitrogen to ammonia at a single molybdenum center. *Science* **2003**, *301*, 76−78.
(19) Betley, T. A.; Peters, J. C. Dinitrogen chemistry from trigonally coordinated iron and cobalt platforms. *J. Am. Chem. Soc.* **2003**, *125*, 10782−10783.
(20) Schrock, R. R. Catalytic reduction of dinitrogen to ammonia by molybdenum: theory versus experiment. *Angew. Chem., Int. Ed.* **2008**, *47*, 5512−5522.
(21) Arashiba, K.; Miyake, Y.; Nishibayashi, Y. A molybdenum complex bearing PNP-type pincer ligands leads to the catalytic reduction of dinitrogen into ammonia. *Nat. Chem.* **2011**, *3*, 120−125.
(22) Rodriguez, M. M.; Bill, E.; Brennessel, W. W.; Holland, P. L. N_2 reduction and hydrogenation to ammonia by a molecular iron-potassium complex. *Science* **2011**, *334*, 780−783.
(23) MacLeod, K. C.; Holland, P. L. Recent developments in the homogeneous reduction of dinitrogen by molybdenum and iron. *Nat. Chem.* **2013**, *5*, 559−565.
(24) Anderson, J. S.; Rittle, J.; Peters, J. C. Catalytic conversion of nitrogen to ammonia by an iron model complex. *Nature* **2013**, *501*, 84−87.
(25) Čorić, I.; Mercado, B. Q.; Bill, E.; Vinyard, D. J.; Holland, P. L. Binding of dinitrogen to an iron−sulfur−carbon site. *Nature* **2015**, *526*, 96−99.
(26) Tanaka, H.; Nishibayashi, Y.; Yoshizawa, K. Interplay between theory and experiment for ammonia synthesis catalyzed by transition metal complexes. *Acc. Chem. Res.* **2016**, *49*, 987−995.
(27) Silantyev, G. A.; Förster, M.; Schluschaß, B.; Abbenseth, J.; Wgrtele, C.; Volkmann, C.; Holthausen, M. C.; Schneider, S. Dinitrogen splitting coupled to protonation. *Angew. Chem., Int. Ed.* **2017**, *56*, 5872−5876.
(28) Ashida, Y.; Arashiba, K.; Nakajima, K.; Nishibayashi, Y. Molybdenum-catalysed ammonia production with samarium diiodide and alcohols or water. *Nature* **2019**, *568*, 536−540.
(29) Haber, F. Ammonia. German patent DE229126, 1909.
(30) Roussel, P.; Scott, P. Complex of dinitrogen with trivalent uranium. *J. Am. Chem. Soc.* **1998**, *120*, 1070−1071.
(31) Odom, A. L.; Arnold, P. L.; Cummins, C. C. Heterodinuclear uranium/molybdenum dinitrogen complexes. *J. Am. Chem. Soc.* **1998**, *120*, 5836−5837.
(32) Cloke, G. F. N.; Hitchcock, P. B. Reversible binding and reduction of dinitrogen by a uranium(III) pentalene complex. *J. Am. Chem. Soc.* **2002**, *124*, 9352−9353.
(33) Korobkov, I.; Gambarotta, S.; Yap, G. P. A highly reactive uranium complex supported by the calix[4] tetrapyrrole tetraanion affording dinitrogen cleavage, solvent deoxygenation, and polysilanol depolymerization. *Angew. Chem., Int. Ed.* **2002**, *41*, 3433−3436.
(34) Evans, W. J.; Kozimor, S. A.; Ziller, J. W. A monometallic f element complex of dinitrogen: $(C_5Me_5)_3U(\eta^1\text{-}N_2)$. *J. Am. Chem. Soc.* **2003**, *125*, 14264−14265.
(35) Mansell, S. M.; Kaltsoyannis, N.; Arnold, P. L. Small molecule activation by uranium tris(aryloxides): experimental and computational studies of binding of N_2, coupling of CO, and deoxygenation insertion of CO_2 under ambient conditions. *J. Am. Chem. Soc.* **2011**, *133*, 9036−9051.
(36) Falcone, M.; Chatelain, L.; Scopelliti, R.; Živković, I.; Mazzanti, M. Nitrogen reduction and functionalization by a multimetallic uranium nitride complex. *Nature* **2017**, *547*, 332−335.
(37) Falcone, M.; Barluzzi, L.; Andrez, J.; Tirani, F. F.; Zivkovic, I.; Fabrizio, A.; Corminboeuf, C.; Severin, K.; Mazzanti, M. The role of bridging ligands in dinitrogen reduction and functionalization by uranium multimetallic complexes. *Nat. Chem.* **2019**, *11*, 154−160.
(38) Lu, J.-B.; Ma, X.-L.; Wang, J.-Q.; Jiang, Y.-F.; Li, Y.; Hu, H.-S.; Xiao, H.; Li, J. The df−d dative bonding in a uranium−cobalt heterobimetallic complex for efficient nitrogen fixation. *Inorg. Chem.* **2019**, *58*, 7433−7439.
(39) Lu, E.; Atkinson, B. E.; Wooles, A. J.; Boronski, J. T.; Doyle, L. R.; Tuna, F.; Cryer, J. D.; Cobb, P. J.; Vitorica-Yrezabal, I. J.; Whitehead, G. F. S.; Kaltsoyannis, N.; Liddle, S. T. Back-bonding between an electron-poor, high-oxidation-state metal and poor π-acceptor ligand in a uranium(V)−dinitrogen complex. *Nat. Chem.* **2019**, *11*, 806−811.
(40) Arnold, P. L.; Ochiai, T.; Lam, F. Y. T.; Kelly, R. P.; Seymour, M. L.; Maron, L. Metallacyclic actinide catalysts for dinitrogen conversion to ammonia and secondary amines. *Nat. Chem.* **2020**, *12*, 654−659.
(41) Fox, A. R.; Bart, S. C.; Meyer, K.; Cummins, C. C. Towards uranium catalysts. *Nature* **2008**, *455*, 341−349.
(42) Feng, G.; Zhang, M.; Shao, D.; Wang, X.; Wang, S.; Maron, L.; Zhu, C. Transition metal bridged bimetallic clusters with multiple uranium-metal bonds. *Nat. Chem.* **2019**, *11*, 248−253.
(43) Feng, G.; Zhang, M.; Wang, P.; Wang, S.; Maron, L.; Zhu, C. Identification of a uranium−rhodium triple bond in a heterometallic cluster. *Proc. Natl. Acad. Sci. U. S. A.* **2019**, *116*, 17654−17658.
(44) Xin, X.; Zhu, C. Isolation of heterometallic cerium(III) complexes with a multidentate nitrogen−phosphorus ligand. *Dalton Trans.* **2020**, *49*, 603−607.
(45) Feng, G.; McCabe, K. N.; Wang, S.; Maron, L.; Zhu, C. Construction of heterometallic clusters with multiple uranium-metal bonds by dianionic nitrogen-phosphorus ligands. *Chem. Sci.* **2020**, *11*, 7585−7592.
(46) Chatelain, L.; Scopelliti, R.; Mazzanti, M. Synthesis and structure of nitride-bridged uranium(III) complexes. *J. Am. Chem. Soc.* **2016**, *138* (6), 1784−1787.
(47) Falcone, M.; Chatelain, L.; Mazzanti, M. Nucleophilic reactivity of a nitride-bridged diuranium (IV) complex: CO_2 and CS_2 functionalization. *Angew. Chem., Int. Ed.* **2016**, *55*, 4074−4078.
(48) Falcone, M.; Kefalidis, C. E.; Scopelliti, R.; Maron, L.; Mazzanti, M. Facile CO cleavage by a multimetallic CsU_2 nitride complex. *Angew. Chem., Int. Ed.* **2016**, *55*, 12290−12294.
(49) Falcone, M.; Poon, L. N.; Tirani, F. F.; Mazzanti, M. Reversible dihydrogen activation and hydride transfer by a uranium nitride complex. *Angew. Chem., Int. Ed.* **2018**, *57*, 3697−3700.
(50) Palumbo, C. T.; Barluzzi, L.; Scopelliti, R.; Zivkovic, I.; Fabrizio, A.; Corminboeuf, C.; Mazzanti, M. Tuning the structure, reactivity and magnetic communication of nitride-bridged uranium complexes with the ancillary ligands. *Chem. Sci.* **2019**, *10*, 8840−8849.
(51) Castro-Rodriguez, I.; Nakai, H.; Zakharov, L. N.; Rheingold, A. L.; Meyer, K. A linear, O-coordinated η^1-CO_2 bound to uranium. *Science* **2004**, *305*, 1757−1759.
(52) Lam, O. P.; Feng, P. L.; Heinemann, F. W.; O'Connor, J. M.; Meyer, K. Charge-separation in uranium diazomethane complexes

https://dx.doi.org/10.1021/jacs.0c05788
J. Am. Chem. Soc. 2020, 142, 15004−15011

leading to C-H activation and chemical transformation. *J. Am. Chem. Soc.* **2008**, *130*, 2806−2816.
(53) Duhovic, S.; Oria, J. V.; Odoh, S. O.; Schreckenbach, G.; Batista, E. R.; Diaconescu, P. L. Investigation of the electronic structure of mono(1,1′-diamidoferrocene) uranium(IV) complexes. *Organometallics* **2013**, *32*, 6012−6021.
(54) Anderson, N. H.; Odoh, S. O.; Williams, U. J.; Lewis, A. J.; Wagner, G. L.; Lezama Pacheco, J.; Kozimor, S. A.; Gagliardi, L.; Schelter, E. J.; Bart, S. C. Investigation of the electronic ground states for a reduced pyridine(diimine) uranium series: evidence for a ligand tetraanion stabilized by a uranium dimer. *J. Am. Chem. Soc.* **2015**, *137*, 4690−4700.
(55) Mills, D. P.; Moro, F.; McMaster, J.; van Slageren, J.; Lewis, W.; Blake, A. J.; Liddle, S. T. A delocalized arene-bridged diuranium single-molecule magnet. *Nat. Chem.* **2011**, *3*, 454−460.
(56) Pyykkö, P.; Atsumi, M. Molecular single-bond covalent radii for elements 1−118. *Chem. - Eur. J.* **2009**, *15*, 186−197.
(57) Hlina, J. A.; Wells, J. A.; Pankhurst, J. R.; Love, J. B.; Arnold, P. L. Uranium rhodium bonding in heterometallic complexes. *Dalton Trans.* **2017**, *46*, 5540−5545.
(58) Lu, E.; Wooles, A. J.; Gregson, M.; Cobb, P. J.; Liddle, S. T. A very short uranium(IV)-rhodium(I) bond with net double-dative bonding character. *Angew. Chem., Int. Ed.* **2018**, *57*, 6587−6591.
(59) Diaconescu, P. L.; Arnold, P. L.; Baker, T. A.; Mindiola, D. J.; Cummins, C. C. Arene-bridged diuranium complexes: inverted sandwiches supported by δ backbonding. *J. Am. Chem. Soc.* **2000**, *122*, 6108−6109.
(60) Kiernicki, J. J.; Ferrier, M. G.; Lezama Pacheco, J. S.; La Pierre, H. S.; Stein, B. W.; Zeller, M.; Kozimor, S. A.; Bart, S. C. Examining the effects of ligand variation on the electronic structure of uranium bis(imido) species. *J. Am. Chem. Soc.* **2016**, *138*, 13941−13951.
(61) Sternal, R. S.; Marks, T. J. Actinide-to-transition metal bonds. Synthesis, characterization, and properties of metal-metal bonded systems having the tris (cyclopentadienyl) actinide fragment. *Organometallics* **1987**, *6*, 2621−2623.
(62) Gagliardi, L.; Roos, B. O. Quantum chemical calculations show that the uranium molecule U_2 has a quintuple bond. *Nature* **2005**, *433*, 848−851.
(63) Knecht, S.; Jensen, H. J. A.; Saue, T. Relativistic quantum chemical calculations show that the uranium molecule U_2 has a quadruple bond. *Nat. Chem.* **2019**, *11*, 40−44.
(64) Napoline, J. W.; Kraft, S. J.; Matson, E. M.; Fanwick, P. E.; Bart, S. C.; Thomas, C. M. Tris(phosphinoamide)-supported uranium−cobalt heterobimetallic complexes featuring Co→U dative interactions. *Inorg. Chem.* **2013**, *52*, 12170−12177.
(65) Gardner, B. M.; McMaster, J.; Lewis, W.; Liddle, S. T. Synthesis and structure of $[\{N(CH_2CH_2NSiMe_3)_3\}URe(\eta^5\text{-}C_5H_5)_2]$: A heterobimetallic complex with an unsupported uranium-rhenium bond. *Chem. Commun.* **2009**, 2851−2853.
(66) Ward, A. L.; Lukens, W. W.; Lu, C. C.; Arnold, J. Photochemical route to actinide-transition metal bonds: Synthesis, characterization and reactivity of a series of thorium and uranium heterobimetallic complexes. *J. Am. Chem. Soc.* **2014**, *136*, 3647−3654.
(67) Hlina, J. A.; Pankhurst, J. R.; Kaltsoyannis, N.; Arnold, P. L. Metal−metal bonding in uranium−group 10 complexes. *J. Am. Chem. Soc.* **2016**, *138*, 3333−3345.
(68) Chi, C.; Wang, J.-Q.; Qu, H.; Li, W.-L.; Meng, L.; Luo, M.; Li, J.; Zhou, M. Preparation and characterization of uranium-iron triple-bonded $UFe(CO)_3^-$ and $OUFe(CO)_3^-$ complexes. *Angew. Chem., Int. Ed.* **2017**, *56*, 6932−6936.

https://dx.doi.org/10.1021/jacs.0c05788
J. Am. Chem. Soc. 2020, 142, 15004−15011